

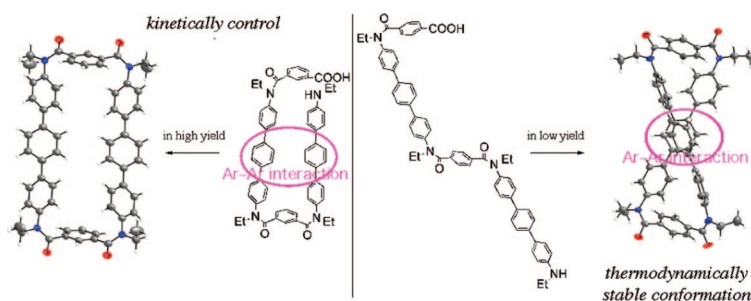
Effect of Aromatic–Aromatic Interactions on the Conformational Stabilities of Macrocycle and Preorganized Structure during Macrocyclization

Kosuke Katagiri, Taichi Tohaya, Hyuma Masu, Masahide Tominaga, and Isao Azumaya*

Faculty of Pharmaceutical Sciences at Kagawa Campus, Tokushima Bunri University,
1314-1 Shido, Sanuki, Kagawa 769-2193, Japan

azumayai@kph.bunri-u.ac.jp

Received January 6, 2009



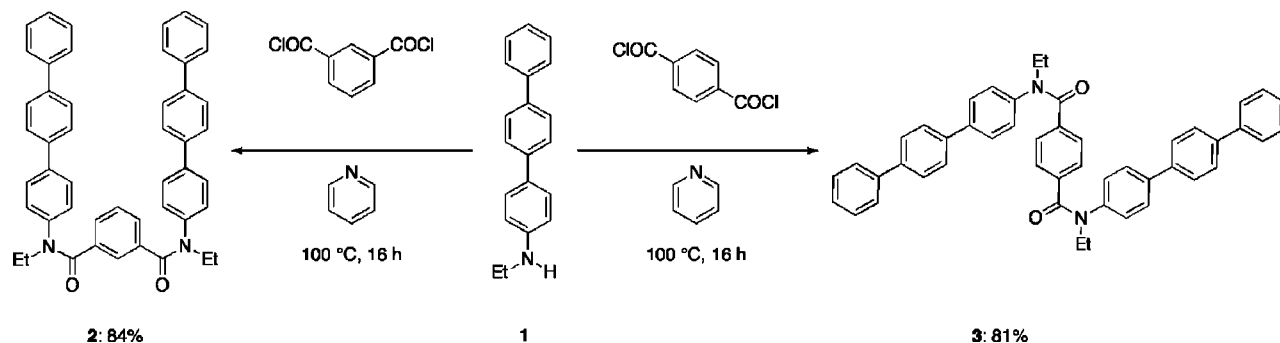
The crystal structures and dynamic behavior in solution of aromatic amides containing terphenyl groups were revealed by X-ray crystallographic analysis and VT-NMR measurements. Controlling the synthetic yield and molecular shape of the macrocycles with intramolecular aromatic–aromatic interactions was successfully achieved. *N,N'*-Diethyl-*N,N'*-diterphenyl-1,3-benzenedicarboxamide (**2**) exists in the *syn* conformation and two terphenyl groups are on the same side of the plane of the central benzene ring due to attractive aromatic–aromatic interactions between the two terphenyl moieties. The yield of the macrocyclization reaction of 1,3-benzenedicarboxylic acid with bis(ethylamino)terphenyl (**4**) was relatively high (55% yield) because an intermediate in the macrocyclization reaction was preorganized in the *syn* conformation, which is similar to the diamide **2**. On the other hand, *N,N'*-diethyl-*N,N'*-diterphenyl-1,4-benzenedicarboxamide (**3**) exists in the *anti* conformation and two terphenyl groups are positioned on opposite sides of the plane of the central benzene ring. In contrast to the 1,3-derivative, the yield of the macrocyclization reaction of the 1,4-benzenedicarboxylic acid with the diamine **4** was low (19% yield). Although macrocycle **5** exists in a planar conformation in the crystal and in solution, macrocycle **6** exists in a twisted conformation. A deformation of the twist was induced by a tilted T-shaped aromatic–aromatic interaction between the central phenylene rings of the macrocycle.

Introduction

Macrocyclic amide compounds have attracted significant attention because of their unique properties, shapes, and applications.¹ The synthetic strategies for preparation of macrocyclic compounds² is based on template synthesis,³ metal-supported self-assembly of small molecules,⁴ and cyclization reactions of preorganized small partial molecules.⁵ These types

of programmed assemblies help to fix the bonding direction and are driven by relatively weak noncovalent interactions such as hydrogen bonding, CH– π interactions, and aromatic–aromatic interactions.⁶ As we reported previously, we found that the *cis* preference of tertiary aromatic amide could be used for effective amidomacrocyclization, that is *N*-alkylaminobenzoic acids was coupled with themselves by a one-step reaction with tetrachlorosilane or dichlorotriphenylphosphorane to give amide macrocycles.⁷ In a large macrocyclic compound synthesis, the rather weak aromatic–aromatic interactions also contribute to a stable intermediate conformation, i.e., induce a preorganized structure. Recently, Fallis's group and Marsella's group reported the correspondence of intramolecular aromatic–aromatic interac-

(1) (a) Gasparini, F.; Pierini, M.; Villani, C.; Filippi, A.; Speranza, M. *J. Am. Chem. Soc.* **2008**, *130*, 522–534. (b) Shah, N. H.; Butterfoss, G. L.; Nguyen, K.; Yoo, B.; Bonneau, R.; Rabenstein, D. L.; Kirshenbaum, K. *J. Am. Chem. Soc.* **2008**, *130*, 16622–16632. (c) Alfonso, I.; Burguete, M. I.; Galindo, F.; Luis, S. V.; Vigarà, L. *J. Org. Chem.* **2007**, *72*, 7947–7956. (d) Huc, I. *Eur. J. Org. Chem.* **2004**, 17–29. (e) Stetter, H.; Marx, J. *Angew. Chem.* **1957**, *69*, 439.

SCHEME 1. The Synthesis of Aromatic Diamides **2** and **3**

tions to the synthetic yield for macrocyclization and the stability of twisted conformation.^{6e,f} During our investigations into the effective synthesis of amide macrocycles, we found that a simple partial structure preorganized by aromatic–aromatic interactions, preferably containing a *syn* conformation of aromatic tertiary diamides, was extremely effective for constructing covalently bonded macrocyclic compounds.⁸ In this paper, we report on the crystal structure and dynamic behavior in solution of aromatic amides with a *p*-terphenyl backbone containing 1,3-

benzenedicarbonyl and 1,4-benzenedicarbonyl moieties. The effect of aromatic–aromatic interactions on the synthetic yield and stable conformation are discussed.

Results and Discussion

Diamides **2** and **3** were synthesized by the reaction of 1,3-benzenedicarbonyl chloride or 1,4-benzenedicarbonyl chloride with *N*-ethylaminoterphenyl **1** (Scheme 1).

X-Ray crystallographic analysis was performed on a single crystal of **2** that was obtained by slow evaporation of a chloroform solution.⁹ The crystal belongs to the space group $P\bar{1}$ (Figure 1), and the unit cell contains four molecules of **2**. Two amide moieties exist in a *syn* conformation, which places the terphenyl groups in the same direction. In this crystal, the intramolecular tilted T-shaped aromatic–aromatic (CH– π) interaction between the two central phenylene rings of both terphenyl groups was observed (Figure 1c).

The single crystals of **3** were also obtained by slow evaporation of a chloroform solution.¹⁰ The crystal belongs to the space group $C2/c$ (Figure 2), and the unit cell contains four molecules of **3**. Two amide moieties exist in a *anti* conformation, which places the terphenyl groups in opposite directions.

To evaluate the dynamic behavior of **2** and **3** in solution, the VT-NMR measurements in dichloromethane-*d*₂ were performed. The different conformers of the diamides (**2**, **3**) would arise from the conformation of the amide groups (*E* or *Z*). Additionally, the torsion angles of the carbonyl planes with the central benzene ring (*syn* or *anti*) and the *N*-terphenyl bond with the amide plane will be different. In these compounds, the *N*-terphenyl rotation can generally be neglected because the rotation of the *N*-terphenyl bonds is fast on the ¹H NMR time scale such that the ortho protons on the *N*-terphenyl group (H_{2b} and H_{3b} in Figure

(2) (a) Borisova, N. E.; Reshetova, M. D.; Ustyynyuk, Y. A. *Chem. Rev.* **2007**, *107*, 46–79. (b) Gibson, S. E.; Lecci, C. *Angew. Chem., Int. Ed.* **2006**, *45*, 1364–1377. (c) Cronin, L. *Annu. Rep. Prog. Chem., Sect. A* **2006**, *102*, 353–378. (d) Li, Z.-T.; Hou, J.-L.; Li, C.; Yi, H.-P. *Chem. Asian J.* **2006**, *1*, 766–778. (e) Aricó, F.; Chang, T.; Cantrill, S. J.; Khan, S. I.; Stoddart, J. F. *Chem. Eur. J.* **2005**, *11*, 4655–4666. (f) Baxter, P. N. W.; Dali-Youcef, R. J. *Org. Chem.* **2005**, *70*, 4935–4953. (g) Rebek, J., Jr. *Angew. Chem., Int. Ed.* **2005**, *44*, 2068–2078. (h) Lagona, J.; Mukhopadhyay, P.; Chakrabarti, S.; Isaacs, L. *Angew. Chem., Int. Ed.* **2005**, *44*, 4844–4870. (i) Chang, K.-J.; Moon, D.; Lah, M. S.; Jeong, K.-S. *Angew. Chem., Int. Ed.* **2005**, *44*, 7926–7929. (j) Badjić, J. D.; Balzani, V.; Credi, A.; Silvi, S.; Stoddart, J. F. *Science* **2004**, *303*, 1845–1849. (k) Albrecht, M. *Chem. Rev.* **2001**, *101*, 3457–3497. (l) Hill, D. J.; Mio, M. J.; Prince, R. B.; Hughes, T. S.; Moore, J. S. *Chem. Rev.* **2001**, *101*, 3893–4012.

(3) (a) Gómez, L.; Company, A.; Fontrodona, X.; Ribas, X.; Costas, M. *Chem. Commun.* **2007**, 4410–4412. (b) Hoss, R.; Vögtle, F. *Angew. Chem., Int. Ed.* **1994**, *33*, 375–384. (c) Greene, R. *Tetrahedron Lett.* **1972**, *13*, 1793–1796.

(4) (a) Chambron, J.-C.; Heitz, V.; Sauvage, J.-P. *J. Chem. Soc., Chem. Commun.* **1992**, 1131–1133. (b) Anderson, H. L.; Sanders, J. K. M. *Angew. Chem., Int. Ed.* **1990**, *29*, 1400–1403.

(5) (a) Zhu, Y.-Y.; Li, C.; Li, G.-Y.; Jiang, X.-K.; Li, Z.-T. *J. Org. Chem.* **2008**, *73*, 1745–1751. (b) Berni, E.; Dolain, C.; Kauffmann, B.; Lger, J.-M.; Zhan, C.; Huc, I. *J. Org. Chem.* **2008**, *73*, 2687–2694. (c) Zhu, J.; Wang, X.-Z.; Chen, Y.-Q.; Jiang, X.-K.; Chen, X.-Z.; Li, Z.-T. *J. Org. Chem.* **2004**, *69*, 6221–6227. (d) Lin, J.-B.-N.; Xu, X.-N.; Jiang, X.-K.; Li, Z.-T. *J. Org. Chem.* **2008**, *73*, 9403–9410. (e) Qin, B.; Chen, X.; Fang, X.; Shu, Y.; Yip, Y. K.; Yan, Y.; Pan, S.; Ong, W. Q.; Ren, C.; Su, H.; Zeng, H. *Org. Lett.* **2008**, *10*, 5127–5130. (f) He, L.; An, Y.; Yuan, L.; Yamato, K.; Feng, W.; Gerlitz, O.; Zheng, C.; Gong, B. *Chem. Commun.* **2005**, 3788–3790. (g) Yuan, L.; Feng, W.; Yamato, K.; Sanford, A. R.; Xu, D.; Guo, H.; Gong, B. *J. Am. Chem. Soc.* **2004**, *126*, 11120–11121. (h) Jiang, H.; Léger, J.-M.; Guionneau, P.; Huc, I. *Org. Lett.* **2004**, *6*, 2985–2988.

(6) (a) Tanatani, A.; Yokoyama, A.; Azumaya, I.; Takakura, Y.; Mitsui, C.; Shiro, M.; Uchiyama, M.; Muranaka, A.; Kobayashi, N.; Yokozawa, T. *J. Am. Chem. Soc.* **2005**, *127*, 8553–8561. (b) Azumaya, I.; Uchida, D.; Kato, T.; Yokoyama, A.; Tanatani, A.; Takayanagi, H.; Yokozawa, T. *Angew. Chem., Int. Ed.* **2004**, *43*, 1360–1363. (c) Cheng, R. P.; Gellman, S. H.; DeGrado, W. F. *Chem. Rev.* **2001**, *101*, 3219–3232. (d) Oh, K.; Jeong, K.-S.; Moore, J. S. *Nature* **2001**, *414*, 889–893. (e) Marsella, M. J.; Wang, Z.-Q.; Reid, R. J.; Yoon, K. *Org. Lett.* **2001**, *3*, 885–887. (f) Collins, S. K.; Yap, G. P. A.; Fallis, A. G. *Org. Lett.* **2000**, *2*, 3189–3192. (g) Nelson, J. C.; Saven, J. G.; Moore, J. S.; Wolyne, P. G. *Science* **1997**, *277*, 1793–1796.

(7) (a) Masu, H.; Okamoto, T.; Kato, T.; Katagiri, K.; Tominaga, M.; Goda, H.; Takayanagi, H.; Azumaya, I. *Tetrahedron Lett.* **2006**, *47*, 803–807. (b) Imabeppu, F.; Katagiri, K.; Masu, H.; Kato, T.; Tominaga, M.; Therrien, B.; Takayanagi, H.; Kaji, E.; Yamaguchi, K.; Kagechika, H.; Azumaya, I. *Tetrahedron Lett.* **2006**, *47*, 413–416. (c) Azumaya, I.; Okamoto, T.; Imabeppu, F.; Takayanagi, H. *Tetrahedron* **2003**, *59*, 2325–2331. (d) Azumaya, I.; Okamoto, T.; Imabeppu, F.; Takayanagi, H. *Heterocycles* **2003**, *60*, 1419–1424. (e) Azumaya, I.; Kagechika, H.; Yamaguchi, K.; Shudo, K. *Tetrahedron Lett.* **1996**, *37*, 5003–5006.

(8) (a) Tominaga, M.; Masu, H.; Katagiri, K.; Azumaya, I. *Tetrahedron Lett.* **2007**, *48*, 4369–4372. (b) Tominaga, M.; Masu, H.; Katagiri, K.; Kato, T.; Azumaya, I. *Org. Lett.* **2005**, *7*, 3785–3787.

(9) Crystal data of **2**: C₄₈H₄₀N₂O₂; *M* = 676.82, triclinic, space group $P\bar{1}$, *a* = 10.391(2) Å, *b* = 19.155(4) Å, *c* = 19.178(4) Å, α = 107.102(2) deg, β = 93.505(3)°, γ = 91.272(2)°, *V* = 3638.3(12) Å³, *Z* = 4, *D*_{calcd} = 1.236 Mg m⁻³, *T* = 120 K, μ (MoK α) = 0.075 mm⁻¹, GOF on *F*² = 0.807, 17831 reflections measured, 13718 unique (*R*_{int} = 0.0236) which were used in all calculations. The final *R*₁ and *wR*₂ (*F*²) were 0.0529 and 0.1302 [*I* > 2 σ (*I*)]. Additional material comprising full details of the X-ray data collection and final refinement parameters including anisotropic thermal parameters and a full list of the bond lengths and angles have been deposited with the Cambridge Crystallographic Data Center in CIF format as supplementary Publication No. CCDC-712723. Copies of the data can be obtained free of charge on application to CCDC, 12 Union Road, Cambridge, CB21EZ, UK, (fax +44 1223 336 033; e-mail deposit@ccdc.cam.ac.uk).

(10) Crystal data of **3**: C₄₈H₄₀N₂O₂·2CHCl₃; *M* = 915.56, monoclinic, space group $C2/c$, *a* = 30.709(5) Å, *b* = 8.472(1) Å, *c* = 18.198(3) Å, β = 111.575(2)°, *V* = 4402(1) Å³, *Z* = 4, *D*_{calcd} = 1.381 Mg m⁻³, *T* = 150 K, μ (MoK α) = 0.434 mm⁻¹, GOF on *F*² = 1.129, 10371 reflections measured, 4405 unique (*R*_{int} = 0.0319) which were used in all calculations. The final *R*₁ and *wR*₂ (*F*²) were 0.0638 and 0.1687 [*I* > 2 σ (*I*)]. Cambridge Crystallographic Data Center Publication No. CCDC-712724.

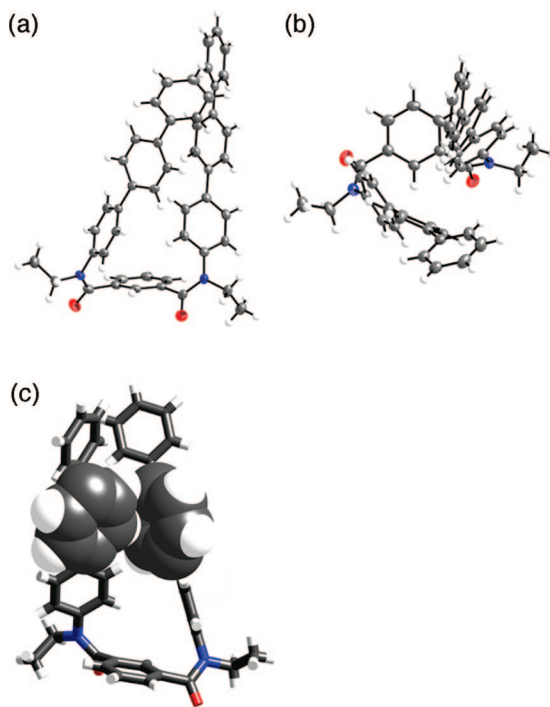


FIGURE 1. The crystal structure of 1,3-diamide terphenyl benzene **2** in the thermal ellipsoids model: (a) front view and (b) top view. (c) Stick model of **2**; the parts of the phenylene units in the middle of the terphenyl group are drawn as a space-filling model. The ring center–ring center distance of the two phenylene groups is 5.244 Å, and the angle between the two phenylene groups is 83.37°.

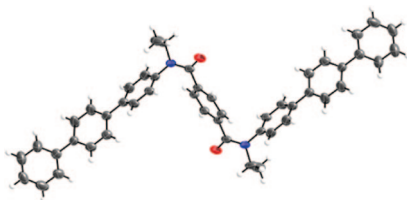


FIGURE 2. The crystal structure of 1,4-diamide terphenyl benzene **3** in the thermal ellipsoids model.

3) are magnetically equivalent. The difference in the chemical shifts between the signals at high and low temperatures indicates that the compositions of different conformational structures (*E/Z* or *syn/anti*, or both) are in fast equilibrium and this equilibrium is temperature dependent. Figure 3 shows the temperature dependence of the ^1H NMR spectra in the aromatic region of diamides **2** and **3**, which are very similar to that of *N,N'*-dimethyl-*N,N'*-diphenyl-1,3- and -1,4-benzenedicarboxamide.¹¹ The chemical shifts of the terphenyl protons (ortho to the amide bond: H_{2b} in Figure 3a) of diamide **2** moved upfield (from 6.97 at 293 K to 6.81 ppm at 173 K) because the ratio of the *syn* conformation that has a higher chemical shift value increased as the temperature was lowered. Furthermore, peak broadening at 253–273 K suggests that there is an equilibrium of a species with a *Z* isomer that exists as a small amount, and the coalescence point of the H_{2b} peaks at 243–253 K is due to the *E/Z* conversion (Figure 3a, $\Delta G^\ddagger = 13.1 \pm 0.3 \text{ kcal mol}^{-1}$). On the other hand, the chemical shifts of the terphenyl protons (ortho to the amide bond: H_{3b} in Figure 3b) of diamide **3** were lower than those of **2** and were temperature independent. This

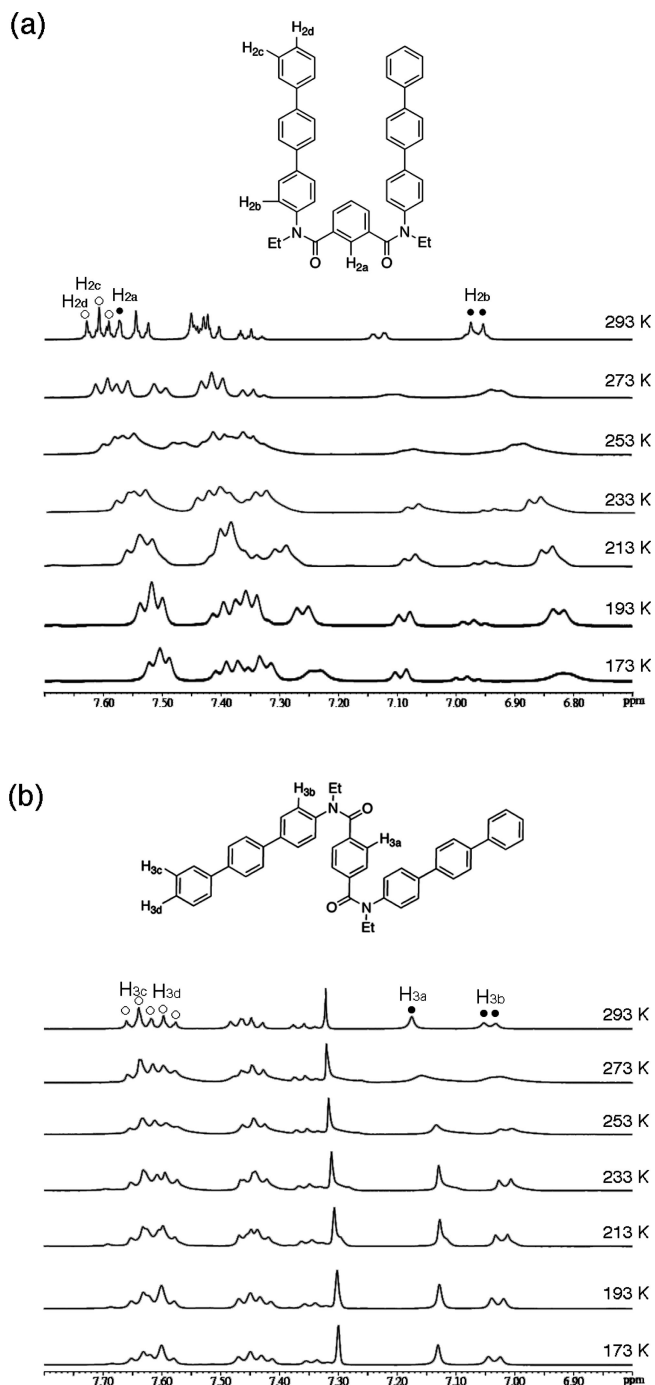


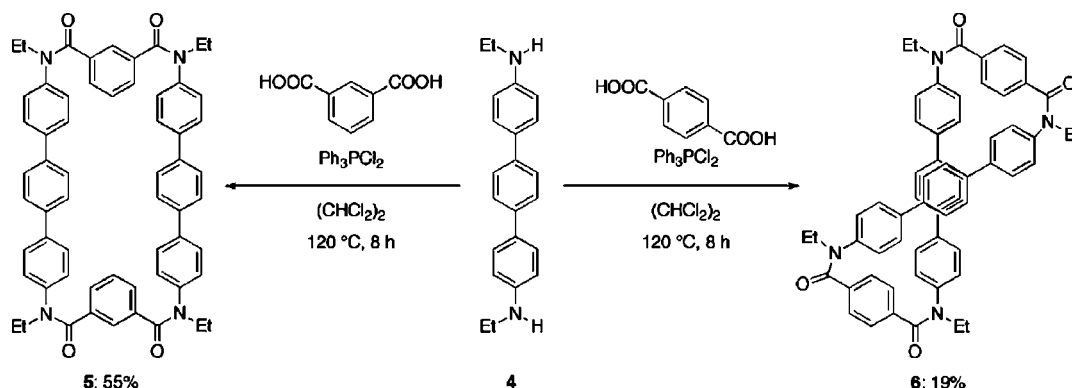
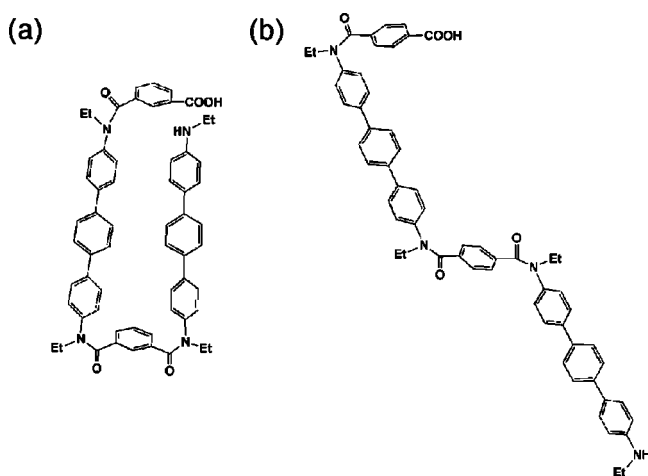
FIGURE 3. (a) The temperature dependence of ^1H NMR signals of **2** in the aromatic region. (b) The temperature dependence of ^1H NMR signals of **3** in the aromatic region.

showed that aromatic–aromatic interactions were faint and this is due to the larger distance between the terphenyl groups.

Next, macrocyclic tetraamide **5** was synthesized by the direct amide coupling of 1,3-benzenedicarboxylic acid with 1,4-bis(4-*N*-ethylaminophenyl)benzene **4**^{8b} by using dichlorotriphenylphosphorane, which has been previously reported to be an effective coupling reagent to construct macrocyclic aromatic amides.¹² A mixture of 1,3-benzenedicarboxylic acid and the diamine **4** (1:1

(11) Azumaya, I.; Kagechika, H.; Yamaguchi, K.; Shudo, K. *Tetrahedron* **1995**, *51*, 5277–5290.

(12) (a) Itai, A.; Toriumi, Y.; Saito, S.; Kagechika, H.; Shudo, K. *J. Am. Chem. Soc.* **1992**, *114*, 10649–10650. (b) Azumaya, I.; Kagechika, H.; Fujiwara, Y.; Itoh, M.; Yamaguchi, K.; Shudo, K. *J. Am. Chem. Soc.* **1991**, *113*, 2833–2838.

SCHEME 2. The Synthesis of a Macrocylic Compound **5** and a Twisted Molecule **6**SCHEME 3. Preorganized Structure during the Formation of the Macrocylic Compounds: (a) the Intermediate of a Condensation of 1,3-Benzenedicarboxylic Acid with **4** Exists in the *syn* Conformation and (b) the Intermediate of a Condensation of 1,4-Benzenedicarboxylic Acid with **4** Exists in the *anti* Conformation

in molar ratio) was treated with 2.4 equiv of Ph_3PCl_2 in 1,1,2,2-tetrachloroethane (50 mM of the amine) at $120\text{ }^\circ\text{C}$ for 8 h. The crude product was purified by silica gel column chromatography (eluent: $\text{CHCl}_3:\text{MeOH} = 10:1$) and gel permeation chromatography to give the macrocyclic aromatic amide **5** with a 55% yield. In contrast to the high yield in the synthesis of **2**, a condensation of 1,4-benzenedicarboxylic acid and the diamine **4** under the same conditions gave macrocyclic tetramide **6** with only a 19% yield (Scheme 2). Furthermore, a reaction of 1,2-benzenedicarboxylic acid and **4** gave a product with the same mass number in only trace amounts, which could not be fully characterized. The difference of the yield of the macrocycles is thought to arise from the major conformation of an intermediate during the reaction. That is, these macrocyclizations would proceed under kinetic control.¹³ In the reaction yielding **5**, the final amide coupling of the intermediate right before the cyclization would proceed easily as the intermediate exists primarily in the *syn* conformation. In contrast, in the reaction yielding **6**, the final amide coupling of the intermediate would not proceed easily because the ratio of the *anti* conformation of the intermediate is higher than that of **5** (Scheme 3). As such, the synthetic yield depended on the preorganized structure of the intermediate, which is induced by intramolecular aromatic–aromatic interactions.

X-Ray crystallographic analysis was performed on a single crystal of **5**, which was obtained from a mixture of chloroform, ethyl acetate, and methanol by slow evaporation of the solvent.¹⁴ The crystal belongs to the space group $P2_1/n$ (Figure 4), and the unit cell contains two molecules of the macrocycle **5**.

In the crystal structure of **5**, weak intermolecular interactions between adjacent molecules were observed and the arrangement of the molecules leads to the formation of a network structure (Figure 5a). The two sets of macrocyclic compound **5** per unit cell alternate along the *b* and *c* axes with C–H \cdots O interactions (Figure 5b). Furthermore, the macrocycles **5** form columnar stacking along the *a* axis with C–H \cdots O interactions (C6–H6 \cdots O1: 2.442 Å) and CH– π interactions (C3–H3 \cdots C13: 2.896 Å) (Figure 5c).

Next, a single crystal of **6** was obtained from a mixture of chloroform, ethyl acetate, and ethanol by slow evaporation of the solvent.¹⁵ The crystal structure of **6** is shown in Figure 6. The intramolecular tilted T-shaped aromatic–aromatic interaction between central phenylene groups of the terphenyl moieties was observed and forces the molecule to form a twisted conformation (Figure 6c). The crystal belonged to the space group $P2_1/c$, which contains two sets of enantiomeric twisted conformers per unit cell. This resulted in the crystal having no optical activity. The unit cell contains 8 molecules of ethanol and 12 molecules of water to fill the space among the macrocycles. The aggregate of a single enantiomer of **6** aligns along the *c* axis, with the enantiomeric rows alternating along both the *a* and *b* axes (Figure 7a), and the racemic rows on the *bc* plane of the macrocycle aligning along the *a* axis (Figure 7b).

To evaluate the dynamic behavior of the macrocyclic aromatic amides **5** and **6** in solution, VT-NMR measurements in di-

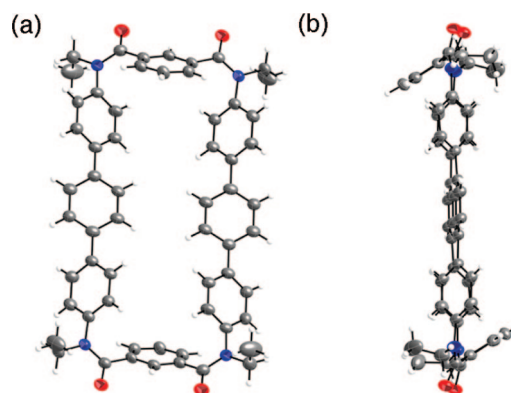


FIGURE 4. The crystal structure of **5** in the thermal ellipsoids model: (a) front view and (b) side view.

(13) Rowan, S. J.; Cantrill, S. J.; Cousins, G. R. L.; Sanders, J. K. M.; Stoddart, J. F. *Angew. Chem., Int. Ed.* **2002**, *41*, 898–952.

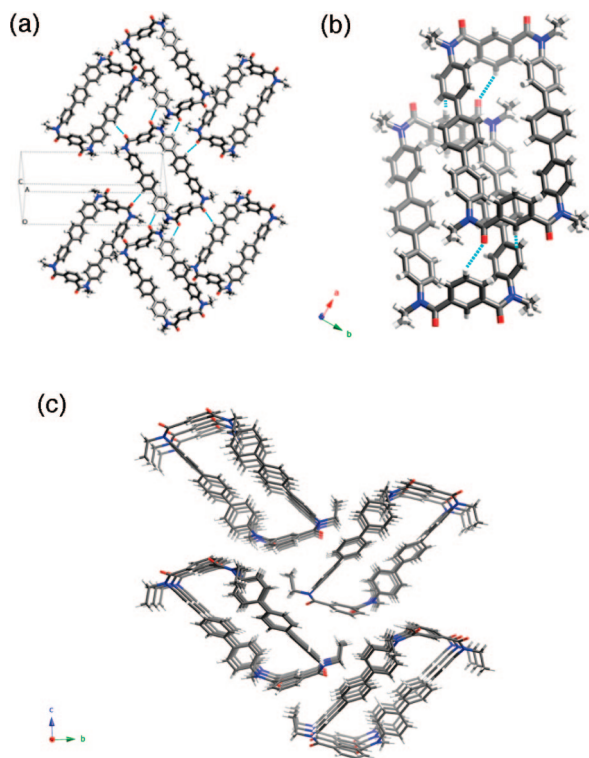


FIGURE 5. (a) Weak interactions (light blue line) with adjacent molecules in the *bc* plane. (b) Weak interactions (light blue line) with adjacent molecules along the *a* axis. (c) Packing diagram of **5** in the stick model, which is viewed along the *a* axis.

chloromethane-*d*₂ were performed (Figure 8). The phenylene protons ortho to the carbonyl groups of **5** are observed as singlets at room temperature (H_{5a} in Figure 8), but the signals broadened and split at 243 K. This observation indicated that the inversion of the phenylene groups at the head parts of the macrocyclic compound **5** (Scheme 4) slowed as the temperature was lowered. Furthermore, the peak broadening of **5** in the aromatic region was observed and suggests that the rotation of the *N*-terphenyl bonds is slower than that of diamide **2**. On the other hand, a single set of signals was observed for macrocycle **6** at both room and low temperatures (see the Supporting Information). This suggested that the tilted T-shaped aromatic–aromatic interactions, which exist between the two central phenylene rings of terphenyl groups, were too weak to keep the twisted conformation of the macrocycle. As such, the equilibrium between the two enantiomeric conformers **6** is fast. Although the prochiral proton signals did not split into two sets of peaks at 183 K, the racemization was definitely slower at low temperatures because the signals broadened as the temperature was lowered.

(14) Crystal data of **5**: $C_{60}H_{52}N_4O_4$; $M = 893.06$, monoclinic, space group $P2_1/n$, $a = 7.765(2)$ Å, $b = 24.472(7)$ Å, $c = 13.084(4)$ Å, $\beta = 101.834(5)^\circ$, $V = 2433.5(12)$ Å³, $Z = 2$, $D_{\text{calcd}} = 1.219$ Mg m⁻³, $T = 150$ K, $\mu(\text{MoK}\alpha) = 0.077$ mm⁻¹, GOF on $F^2 = 0.946$, 14448 reflections measured, 5493 unique ($R_{\text{int}} = 0.0980$) which were used in all calculations. The final R_1 and wR_2 (F^2) were 0.0874 and 0.2175 [$I > 2\sigma(I)$]. Cambridge Crystallographic Data Center Publication No. CCDC-688290.

(15) Crystal data of **6**: $C_{64}H_{64}N_4O_8$; $M = 1033.19$, monoclinic, space group $P2_1/c$, $a = 16.925(3)$ Å, $b = 15.637(3)$ Å, $c = 22.381(4)$ Å, $\beta = 103.617(4)^\circ$, $V = 5756.8(19)$ Å³, $Z = 4$, $D_{\text{calcd}} = 1.192$ Mg m⁻³, $T = 150$ K, $\mu(\text{MoK}\alpha) = 0.080$ mm⁻¹, GOF on $F^2 = 0.986$, 17239 reflections measured, 5188 unique ($R_{\text{int}} = 0.1071$) which were used in all calculations. The final R_1 and wR_2 (F^2) were 0.0797 and 0.2193 [$I > 2\sigma(I)$]. Cambridge Crystallographic Data Center Publication No. CCDC-688291.

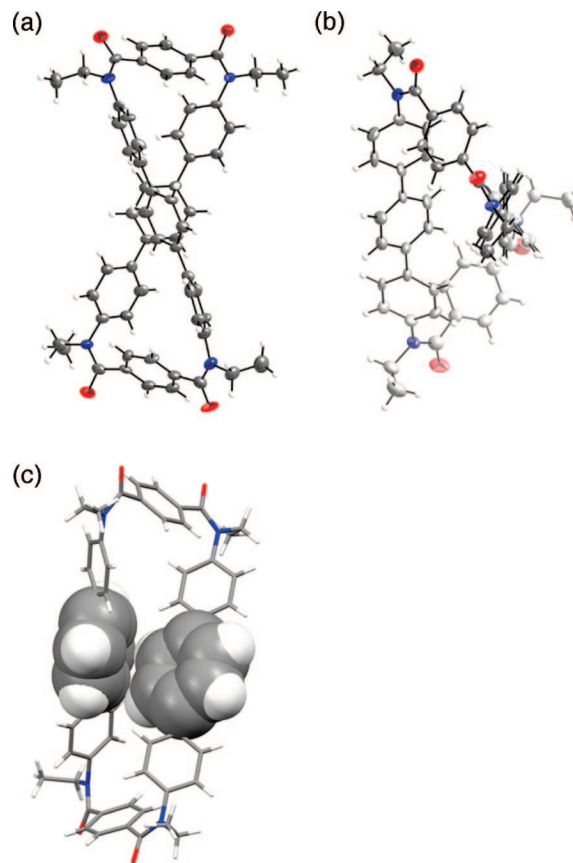


FIGURE 6. The crystal structure of **6** in the thermal ellipsoids model: (a) front view and (b) top view. (c) Stick model of **6**; the parts of the phenylene units in the middle of the terphenyl group are drawn as space-filling models. The hydrogen atom—the ring center distance of the two phenylene groups is 3.153 Å.

Conclusions

In conclusion, the yield of the macrocyclization reaction of 1,3-benzenedicarboxylic acid with bis(ethylamino)terphenyl (**4**) produced a high yield because *N,N'*-diethyl-*N,N'*-diterphenyl-1,3-benzenedicarboxamide **2**, which corresponded to an intermediate on the macrocyclization, existed in the *syn* conformation due to attractive aromatic–aromatic interactions between the two closely positioned terphenyl groups. Conversely, the yield of the macrocyclization reaction of 1,4-benzenedicarboxylic acid with bis(ethylamino)terphenyl (**4**) was relatively low because *N,N'*-diethyl-*N,N'*-diterphenyl-1,4-benzenedicarboxamide (**3**) existed in the *anti* conformation and the two terphenyl groups were located on opposite sides. The meta-macrocyclic **5** existed in a planar conformation and the para-macrocyclic **6** existed in a twisted conformation. A deformation of the twist in **6** was induced by a tilted T-shaped aromatic–aromatic interaction between the central phenylene rings of the macrocycle. That is, the aromatic–aromatic interaction works effectively on the intermediate of the macrocyclization in the meta-macrocyclic synthesis and on the ground state conformation for the para-macrocyclic **6**. We are now exploring various macrocycles with interesting topological properties. Here, the effects of intramolecular aromatic–aromatic interactions on both the synthetic yield and the stability of the conformations are being examined.

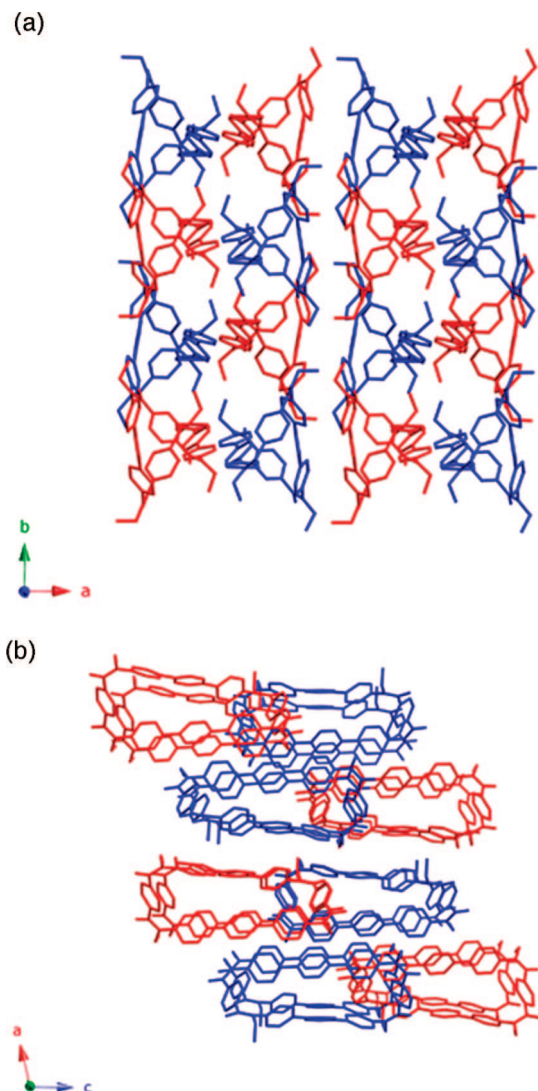


FIGURE 7. Packing diagram of **6** in a stick model presentation. The solvent molecules and hydrogen atoms are omitted for clarity, and the enantiomeric conformations are shown in red and blue, respectively. (a) View along the *c* axis. (b) Projection on the *ac* plane of the unit cell of **6**.

Experimental Section

4'-N-Ethylaminophenyl-4-phenylbenzene (1). Pd/C (10%) was slowly added to a solution of 4-nitro-*p*-terphenyl (1.09 mmol) in dry ethanol (100 mL) with stirring for 4 h under H₂. Acetonitrile (285 μ L) and molecular sieves, which were activated, were added with stirring for 20 h. The Pd/C was filtered and the solvent was removed under reduced pressure. The crude products were purified by silica gel column chromatography (eluent: chloroform) to give **1** in 21% yield as white powder: mp 213 °C; ¹H NMR (400 MHz, CDCl₃) δ 7.64–7.59 (m, 6H), 7.52–7.50 (m, 2H), 7.46–7.42 (m, 2H), 7.36–7.31 (m, 1H), 6.82 (d, *J* = 8.8 Hz, 2H), 3.24 (q, *J* = 7.2 Hz, 2H), 1.31 ppm (t, *J* = 7.2 Hz, 3H); ¹³C NMR (400 MHz, CDCl₃) δ 140.92, 140.17, 138.87, 128.76, 127.86, 127.39, 127.09, 126.95, 126.57, 113.50, 38.92, 14.74 ppm; FAB-MS *m/z* 273.15. Anal. Calcd for C₂₀H₁₉N·¹/₆H₂O: C, 86.92; H, 7.05; N, 5.07. Found: C, 86.90; H, 7.09; N, 5.08.

Bis-1,3-(N-ethyl-N-terphenylamino)carboxybenzene (2). 1,3-Benzenedicarbonyl chloride (0.283 mmol) was slowly added to a solution of 4-*N*-ethylamino-*p*-terphenyl (**1**) (0.566 mmol) in pyridine (5.6 mL) with stirring for 2 h at 100 °C. After 2 h, 1,3-benzenedicarbonyl chloride (0.029 mmol) was added to the reaction

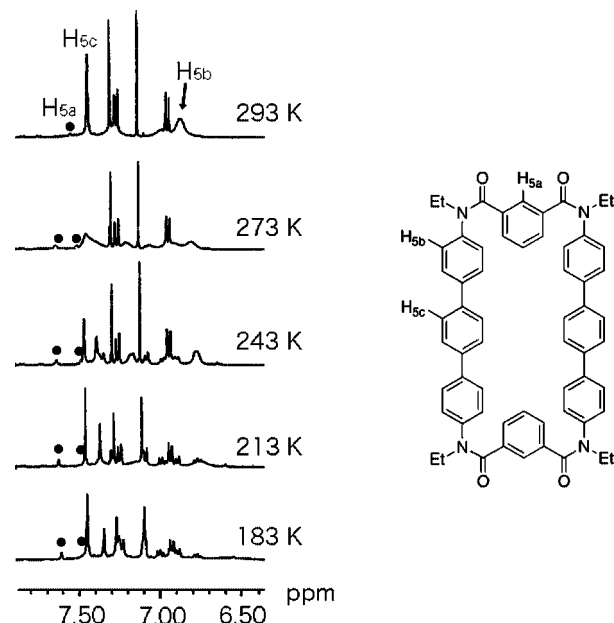
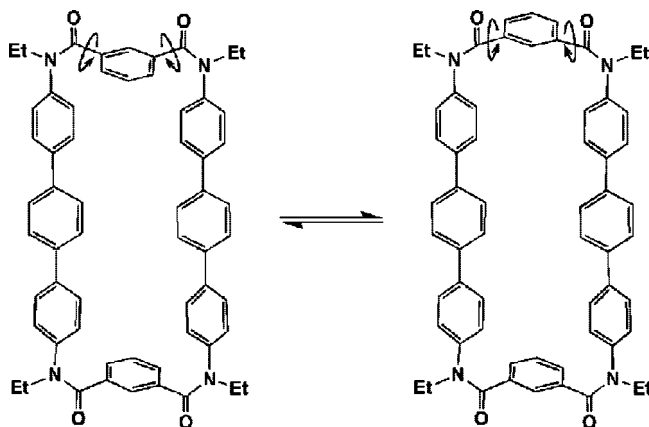


FIGURE 8. The temperature dependence of ¹H NMR signals of **5** in the aromatic region.

SCHEME 4. The Inversion of the *m*-Phenylene Groups of Macrocycle **5**



mixture, and then the solution was heated at 100 °C for 8 h. The mixture was poured into water and extracted with chloroform. The organic layer was dried (Na₂SO₄) and evaporated to give a crude product, which was purified by silica gel column chromatography (eluent: chloroform) to give **2** in 84% yield as a white powder: mp 273–274 °C; ¹H NMR (400 MHz, CDCl₃) δ 7.61–7.49 (m, 6H), 7.37–7.32 (m, 5H), 7.14–7.11 (m, 1H), 6.93 (d, *J* = 8.4 Hz, 3H), 3.95 (q, *J* = 7.2 Hz, 2H), 1.22 ppm (t, *J* = 7.2 Hz, 3H); ¹³C NMR (400 MHz, CDCl₃) δ 169.53 (C = O), 142.30, 140.42, 140.36, 138.74, 138.55, 136.40, 129.40, 129.29, 128.86, 128.20, 127.58, 127.44, 127.17, 126.96, 45.34, 13.02 ppm; FAB-MS *m/z* 676.31. Anal. Calcd for C₄₈H₄₀N₂O₂·¹/₁₄CHCl₃: C, 84.24; H, 5.89; N, 4.09. Found: C, 84.33; H, 5.84; N, 4.11.

Bis-1,4-(N-ethyl-N-terphenylamino)carboxybenzene (3). 1,3-Benzenedicarbonylchloride (0.183 mmol) was slowly added to a solution of 4-*N*-ethylamino-*p*-terphenyl (**1**) (0.366 mmol) in pyridine (3.6 mL) with stirring for 2 h at 100 °C. After 2 h, 1,3-benzenedicarbonyl chloride (0.029 mmol) was added to the reaction mixture, and then it was heated at 100 °C for 8 h. The mixture was poured into water and extracted with chloroform. The organic layer was dried (Na₂SO₄) and evaporated to give a crude product, which was purified by silica gel column chromatography (eluent: chloroform) to give **3** in 81% yield as white powder: mp 229–231 °C;

¹H NMR (400 MHz, CDCl₃) δ 7.56–7.54 (m, 6H), 7.46–7.33 (m, 5H), 7.17 (s, 1H), 7.00 (d, *J* = 8.4 Hz, 3H), 3.94 (q, *J* = 7.2 Hz, 2H), 1.21 ppm (t, *J* = 7.2 Hz, 3H); ¹³C NMR (400 MHz, CDCl₃) δ 169.36 (C=O), 140.48, 140.40, 139.04, 138.62, 137.26, 128.85, 128.24, 128.07, 127.59, 127.53, 127.46, 127.29, 127.01, 45.49, 12.95 ppm; FAB-MS *m/z* 676.31. Anal. Calcd for C₄₈H₄₀N₂O₂·1/11CHCl₃: C, 83.99; H, 5.88; N, 4.07. Found: C, 83.93; H, 5.95; N, 4.05.

Macrocyclic Aromatic Amide 5. To a solution of 1,4-bis(4-*N*-ethylaminophenyl)benzene (**4**) (120 mg, 0.38 mmol) and a 1,3-dicarboxylic acid (63.1 mg, 0.38 mmol) in 1,1,2,2-tetrachloroethane (7.6 mL) under argon was added dichlorotriphenylphosphorane (608 mg, 1.82 mmol) with stirring. The mixture was heated at reflux for 8 h, then the reaction mixture was poured into ice and extracted with ethyl acetate. The organic layer was washed with 4 M HCl, saturated aqueous NaHCO₃, and brine, dried (Na₂SO₄), and evaporated to give a crude product, which was purified by silica gel column chromatography (eluent: CHCl₃:MeOH = 10:1) and preparative gel permeation chromatography using JAIGEL-2H and JAIGEL-2.5H column with chloroform as the mobile phase to give the macrocycle **5** in 55% yield as a white powder: mp >300 °C dec; ¹H NMR (400 MHz, CDCl₃, 27 °C) δ 7.58 (s, 2H), 7.44 (s, 8H), 7.28 (d, *J* = 8.4 Hz, 8H), 7.04 (d, *J* = 7.2 Hz, 4H), 6.91 (d, *J* = 8.0 Hz, 2H), 6.86 (d, *J* = 8.4 Hz, 8H), 3.98 (br s, 8H), 1.24 ppm (t, *J* = 7.2 Hz, 12H); ¹³C NMR (400 MHz, CDCl₃) δ 170.07, 142.41, 138.60, 137.90, 137.24, 128.68, 128.46, 128.06, 127.19, 127.12, 45.02, 12.95 ppm; FAB-MS *m/z* 893.4; ESI-HRMS *m/z* found 892.4011, calcd for C₆₀H₅₂N₄O₄ *m/z* 892.3989. Anal. Calcd for C₆₀H₅₂N₄O₄·3H₂O: C, 78.63; H, 6.00; N, 6.11. Found: C, 78.55; H, 5.89; N, 6.04.

Twisted Macrocyclic Aromatic Amide 6. To a solution of 1,4-bis(4-*N*-ethylaminophenyl)benzene (**4**) (120 mg, 0.38 mmol) and a 1,4-dicarboxylic acid (63.1 mg, 0.38 mmol) in 1,1,2,2-tetrachloroethane (7.6 mL) under argon was added dichlorotriphenylphosphorane (608 mg, 1.82 mmol) with stirring. The mixture was heated at reflux for 8 h, then the reaction mixture was poured into ice and extracted with ethyl acetate. The organic layer was washed with 4 M HCl, saturated aqueous NaHCO₃, and brine, dried (Na₂SO₄), and evaporated to give a crude product, which was purified by silica gel column chromatography (eluent: CHCl₃:MeOH = 10:1) and preparative gel permeation chromatography using JAIGEL-2H and JAIGEL-2.5H column with chloroform as the mobile phase to give the macrocycle **6** in 19% yield as a white powder: mp >300 °C dec; ¹H NMR (400 MHz, CDCl₃, 27 °C) δ 7.32 (s, 8H), 7.28 (d, *J* = 8.6 Hz, 8H), 7.19 (s, 8H), 6.96 (d, *J* = 8.4 Hz, 8H), 3.97 (q, *J* = 7.0 Hz, 8H), 1.21 ppm (t, *J* = 7.0 Hz, 12H); ¹³C NMR (400 MHz, CDCl₃) δ 162.29, 142.23, 139.05, 138.74, 137.38, 128.10, 128.08, 127.37, 127.30, 45.37, 12.87 ppm.; FAB-MS *m/z* 893.4; ESI-HRMS *m/z* found 892.3991, calcd for C₆₀H₅₂N₄O₄ *m/z* 892.3989. Anal. Calcd for C₆₀H₅₂N₄O₄·8H₂O: C, 77.86; H, 6.06; N, 6.05. Found: C, 77.60; H, 5.69; N, 6.06.

Acknowledgment. K.K. is grateful for a Grant-in-Aid for Young Scientists (Start-up), Japan (No. 18890226).

Supporting Information Available: Copies of ¹H and ¹³C NMR spectroscopic data (PDF) and crystallographic analysis data. This material is available free of charge via the Internet at <http://pubs.acs.org>.

JO802801N